Modeling light propagation through taper-microfiber structures integrated on substrates

Xufeng Kou (寇煦丰)[1,a], Guillaume Vienne (范固廉)[1*,b], and Guanghui Wang (王光辉)[2]

[1]*State Key Laboratory of Modern Optical Instrumentation, Department of Optical Engineering, Zhejiang University, Hangzhou 310027, China*

[2]*School of Electrical and Electronic Engineering, Nanyang Technological University, Singapore 639798, Singapore*

[*]*E-mail: guillaumevienne@gmail.com*

Received November 26, 2009

We use the three-dimensional finite-difference time-domain (3D-FDTD) method to model silica taper-microfiber structures integrated on substrates. The dependence of the transmission on the length of the microfiber is investigated for two different structures. Optimization of the geometric parameters is provided and two substrate materials, namely MgF_2 and fluorosilicate glass, are considered. We also investigate the case where the structure is covered with a dielectric material.

OCIS codes: 060.2310, 350.3950, 999.9999 (nanofiber).

doi: 10.3788/COL20100806.0560.

Microfibers offer a promising photonic platform thanks to their simple fabrication process[1−6], ultra-low loss[1,3,5], large evanescent field[7−8], and favorable characteristics for nonlinear optics[9−12]. However, microfibers are easily affected by ambient dust and vibrations. Therefore, developing methods to improve their stability and reliability are crucial to the adoption of microfiber devices. This need has been tackled in recent experimental work[13−19]. One promising way is to integrate such devices on a substrate but, to the best of our knowledge, simulations of this type of structures have not been reported so far.

In this letter, we model the light propagation through taper-microfiber structures integrated on a substrate by means of the three-dimensional finite-difference time-domain (3D-FDTD) method. The simulation is carried out with FullWAVE^{TM}, a commercially available software from RSoft Inc. We optimize the structural parameters to minimize the propagation loss. We study two kinds of structures differing by the way the microfiber is in contact with the substrate, and we discuss the loss mechanisms while comparing two kinds of substrate materials. This may provide valuable references for constructing compact photonic circuits based on optical microfibers.

The basic structure considered here consists of a biconical taper with its central part, the microfiber, lying on a low refractive index plate. Although this basic configuration is simple, it can serve in a variety of practical devices such as supercontinuum sources or sensors. Moreover, the insight gained from this basic configuration can help designing the integration of more complex structures such as interferometers[15] or resonators[16] on substrates. We set out two cases which differ by the way the microfiber lies on the substrate. Figure 1 schematically illustrates the two structures studied in this letter. The two sections of fiber on each side of the biconical taper are placed on a substrate along the same axis, denoted as z-axis. Part of the microfiber is curved and rests on the substrate.

We define the diameter of the microfiber as d, the length of the microfiber along the z-axis as L_c, the wide end of the taper as D, and the length of the taper region as L_t. Initially, we consider the case where the microfiber comes into contact with the substrate only in its middle point. This geometry, which we designate as Structure Type 1, is illustrated in Fig. 1(a). Assuming that the structure is symmetric with respect to the contact point, and further assuming the symmetry as shown in Fig. 1(d), the shape of the microfiber can be considered as a series of four arcs. Structure Type 2, as illustrated in Fig. 1(b), differs from Structure Type 1 in that only a part of the microfiber of length L_c is curved, while the central part of the microfiber of length L_s is straight and lies in contact with the substrate.

The computational domain is set into a uniform orthogonal 3D mesh with grid size of 1/15 of the wavelength which is chosen as 1.55 μm (the telecommunication wavelength) and it is terminated by perfectly matched layers (PMLs)[20]. At this wavelength, the refractive index of silica is 1.444. This is the value used for the microfiber throughout this study, neglecting the influence of the very small amount of germanium found in its center when it is drawn from a standard fiber. We consider that the

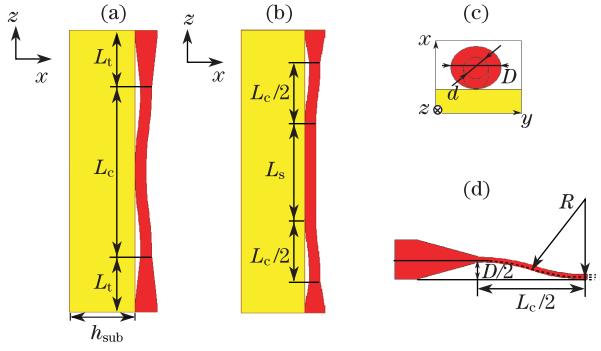

Fig. 1. Geometrical model for 3D-FDTD simulation of the structure. (a) Lateral profile of Structure Type 1; (b) lateral profile of Structure Type 2; (c) x-y cross-section profile; (d) detailed description of the curved microfiber in Structure Type 1.

light is launched into the fundamental mode with the electric field polarized along the x-axis. The presence of the substrate breaks the rotational symmetry along the fiber axis. Therefore, unlike in the case of a microfiber in air, the transmission is expected to be polarization dependent. However, because the ratio of microfiber diameter to the incident wavelength is about 1.7 in our simulation, the evanescent field around the microfiber is very weak (about 5% of the power is guided outside the microfiber). So the asymmetric effect induced by the substrate is limited. For example in the configuration illustrated in Fig. 2(c), the propagation loss is only about 2% lower when the electric field (E-field) is directed along the y-axis compared to when it is along the x-axis. We have checked that the trends studied below remain the same for both polarizations.

The output transmission depends on the geometric parameters of the taper-microfiber structure, namely D, d, L_c, and L_t. Therefore, in order to maximize the transmission, we have to optimize these four parameters.

We choose MgF_2 as the substrate material since it provides a low refractive index[21] (around 1.371 at a wavelength of 1.55 μm) and it is readily available. The basic rule for our parameter optimization is to obtain a good compromise between transmission and structure miniaturization.

By scanning the parameter d from 1.1 to 3.5 μm in Structure Type 1, we observe that the output transmission increases steadily with d until d is above 2.6 μm, where the transmission reaches the plateau at a value around 0.91. The major loss here is caused by the x-axis component of the wave vector $\boldsymbol{k}$ at the contact point between the curved fiber and substrate, where radiation to the substrate occurs. Therefore, we choose d = 2.6 μm as the microfiber's diameter for later simulations.

We then assume a linear taper profile, and find that the output transmission remains almost the same when the ratio of D to d is between 1.5 and 2. We thus choose D as 5 μm. Later, we adjust the ratio of L_t to D from 0.5 to 6; it is shown that the launched light couples almost entirely into the microfiber when this ratio is above 2. To keep the taper short while maintaining a high transmission, we therefore set this ratio to 2, giving L_t = 10 μm in our structure.

The length of the microfiber is a key parameter which greatly influences the light propagation. If we assume that the absorption coefficient of the microfiber is negligible[3], two mechanisms contribute to the total propagation loss: the bending loss of the curved fiber, and the light leakage from the microfiber into the substrate.

To better understand these two factors, we compare two different substrate materials: MgF_2 with a refractive index of 1.371, and a fluorosilicate glass which has a refractive index of 1.423. The latter value is typical for fluorosilicate glasses fabricated by a plasma process, a non-equilibrium process known to be the most efficient for fluorine doping of silicate glasses[22]. In both cases, we choose the geometrical parameters as d = 2.6 μm, D = 5 μm, and L_t = 10 μm, which are optimized for the MgF_2 substrate, but not for the fluorosilicate glass substrate, and we scan L_c from 15 to 100 μm with an increment of ΔL_c = 5 μm. This set of parameters ensures a low light leakage on the MgF_2 substrate as discussed above, but leads to a significant light leakage on the fluorosilicate glass substrate due to the reduced refractive index contrast. This allows us to investigate the importance of the light leakage mechanism in our structures. Figure 2 shows the power distribution along the z-axis and across two cross-sections (at the middle point and the output of the curved fiber). We observe that when L_c is below 50 μm, the radius of curvature of the microfiber is small enough to cause bending loss, which strongly affects the propagation field along the microfiber. For example, in Fig. 2(b), we can see that the power distribution is well-confined and peaks around the center of the microfiber at the middle point (z = 17.5 μm) whereas it is more spread out and off-centered at the output (z = 25 μm). If the substrate is the fluorosilicate glass, the output transmission increases initially with L_c and reaches its peak when L = 50 μm. It then decreases substantially with increasing L_c. This is in sharp contrast with the case of the MgF_2 substrate, where the output transmission increases slightly when L_c is above 50 μm.

The dependence of the transmission on L_c can be explained by the fact that light can leak from the microfiber into the substrate in two ways, which have opposite dependence on L_c. When L_c increases, on one hand, a larger part of the microfiber gets close to the substrate, which causes a larger light leakage to the substrate. On the other hand, the light is launched more parallel to the substrate (in wave picture, the propagation constant β

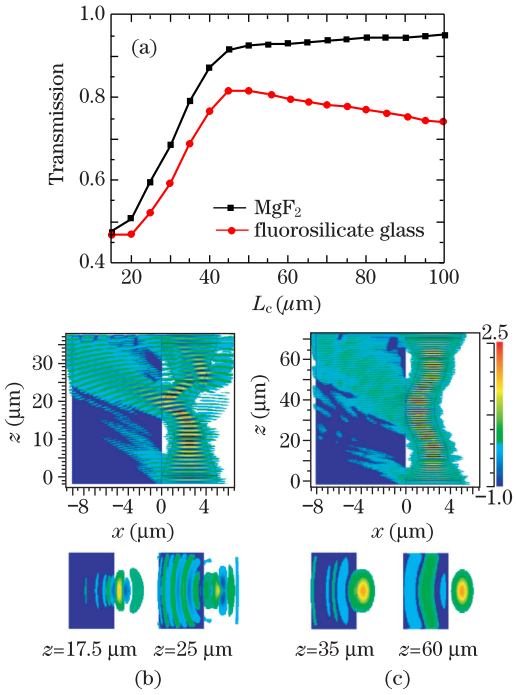

Fig. 2. (a) Transmission of taper-fiber structure versus microfiber length for the MgF_2 and the fluorosilicate glass substrates. Power distributions with two different microfiber lengths on the MgF_2 substrate for (b) L_c = 15 μm and (c) L_c = 50 μm. The other parameters are chosen as d = 2.6 μm, D = 5 μm, L_t = 10 μm, wavelength λ = 1.55 μm, and refractive index of the fiber core n_{core} = 1.444. In (b) and (c), the upper graphs show cross-sections in the x-z plane for y=0, the lower graphs show cross-sections in the x-y plane at the contact point to the substrate (middle of the microfiber) and at the exit of the microfiber.

comes closer to the value of the wave vector $\boldsymbol{k}$), which reduces the propagation along the x-axis and thereby reduces the light leakage to the substrate. When the refractive index difference Δn is small, as for the fluorosilicate glass (Δn= 0.021), the first loss mechanism is significant due to the non-optimized (too small) diameter of the microfiber, and over the optimum length for transmission the leakage to the substrate increases with increasing L_c. However, when the MgF_2 substrate is used, the index difference (Δn = 0.074) is large enough for the leakage to the substrate to be negligible. In fact, we have checked that even for a microfiber 2.6 μm in diameter and 50 μm in length lying straight over a MgF_2 substrate, the transmission is as high as 0.96.

So far, we have modeled the microfiber as a combination of four arcs, corresponding to the microfiber coming into contact with the substrate only at its middle point. However, it is likely to come into contact with the substrate over an extended region. Therefore, we extend our simulations so that the microfiber now consists of four arcs and one straight waveguide in the middle. It is schematically illustrated in Fig. 1(b).

We scan the length of the straight fiber from 0 to 65 μm with the increment value ΔL_s = 5 μm, while maintaining the total length of the microfiber $L = L_c + L_s$ =80 μm. In practice, this value is limited by the available computer memory. As above, we use two different substrates, namely MgF_2 and a fluorosilicate glass. The results are shown in Fig. 3.

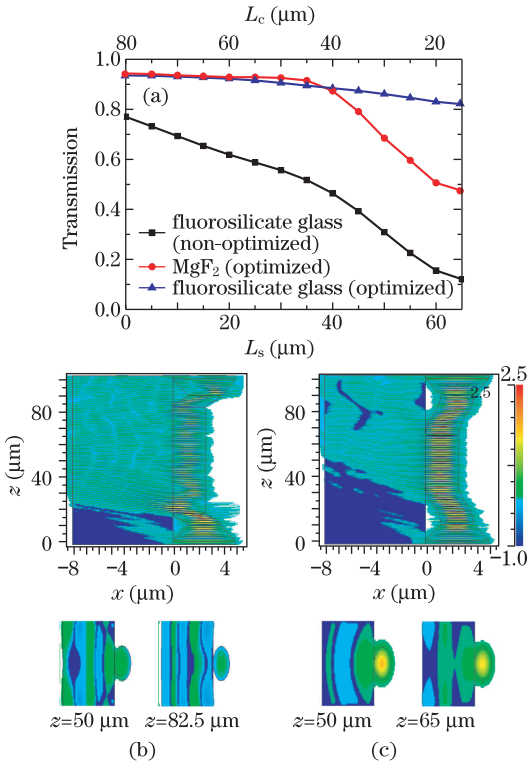

Fig. 3. (a) Transmission of Structure Type 2 versus length for two different substrates. Power distribution when refractive index of the substrate n_{sub} = 1.37 for two different straight microfiber lengths (b) L_s = 65 μm and (c) L_s =30 μm. The other parameters are chosen as d = 2.6 μm, d (optimized for fluorosilicate glass) = 4.0 μm, D = 5 μm, L_t = 10 μm, $L = L_s + L_c$ = 80 μm, λ = 1.55 μm, and n_{core} = 1.444. In (b) and (c), the upper graphs show cross-sections in the x-y plane for $y = 0$, the lower graphs show cross-senctions in the x-z plane at the middle-point and at the end-point of the microfiber-substrate contact region.

For the MgF_2 case, comparing Figs. 2 and 3, we observe that for the same value of L_c in Structures Type 1 and 2, the transmission results are the same. In other words, the additional L_s in Structure Type 2 comes at no cost in terms of transmission.

In Fig. 3, for the fluorosilicate glass substrate, we compare two different structural parameter sets: one is the same as that of the MgF_2 case, and the other is optimized for the fluorosilicate glass substrate, namely d = 4 μm, D = 5 μm, L_t = 10 μm. It can be seen that the fluorosilicate substrate can provide as high a transmission as the MgF_2 substrate, albeit for a larger microfiber diameter of 4.0 μm. This is in sharp contrast with the case where the microfiber diameter is chosen as 2.6 μm, which leads to high transmission for the MgF_2 substrate but low transmission for the fluorosilicate substrate. Clearly, the microfiber diameter must be increased when the refractive index difference between the microfiber and the substrate is reduced.

Cladding a microfiber structure with a dielectric material is beneficial to its mechanical and chemical stability[1,17−19,23]. In this letter, we choose a cladding material with a refractive index of about 1.37 (commercially available fluoropolymers can provide a refractive index as low as 1.29). As before, two kinds of substrates, namely MgF_2 and a fluorosilicate glass, are chosen. It should be noticed that using MgF_2 as a substrate and a cladding material of the same refractive index is optically analog to embedding the structure in a homogeneous material.

We choose Structure Type 1 as the simulation model and the results are shown in Fig. 4. We observe that the transmission curve in the case of MgF_2 has a minimum point at L_c = 35 μm. By comparing the power distribution maps in Figs. 4(b) and (c), it is clear that although the propagation field changes dramatically due to the small bending radius at smaller L_c, it is partially recollected at the output before spreading into the substrate. On the other hand, when L_c = 35 μm, although the bending loss is smaller than for lower values of L_c, the recollection at the output is decreased. Besides, when the substrate material is the fluorosilicate glass, the transmission shows a trend similar to that of MgF_2, but it only slightly increases with L_c above its minimum value at 40 μm. The radiation to the substrate is indeed large as the microfiber is not optimized for the fluorosilicate glass substrate.

Comparing Figs. 2(b) and 4(b), we find that the light recollection is not effective when the structure is exposed to air. This can be attributed to the asymmetry in the refractive index difference on both sides of the contacting surface, which favors leakage of light to the substrate.

In conclusion, we have investigated the light propagation in taper-microfiber structures integrated on different substrates using the 3D-FDTD method. Optimized structural parameters in terms of propagation loss and miniaturization are obtained when MgF_2 is chosen as the substrate. The propagation loss mechanisms, including both bending loss and light leakage from the microfiber to the substrate, have been discussed in detail when

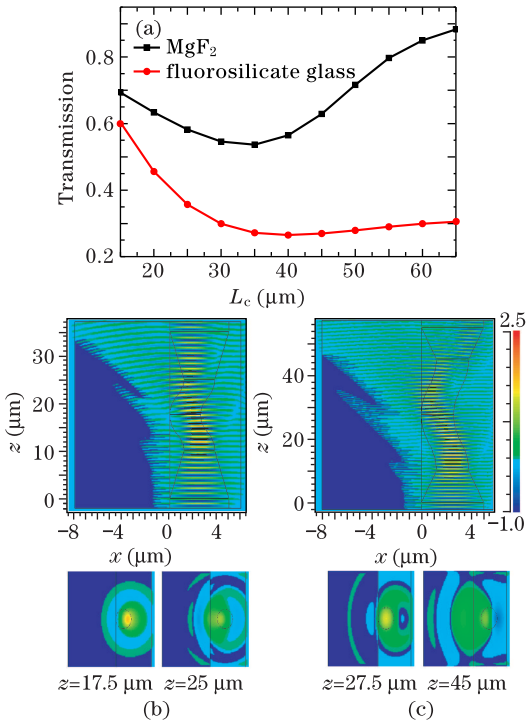

Fig. 4. (a) Transmission of taper-fiber structure versus L_c when it is covered with halogenated polymer (n = 1.37) on MgF_2 (n = 1.37) and on the fluorosilicate glass (n = 1.423) substrates. Power distributions for two different microfiber lengths on the MgF_2 substrate: (b) L_c = 15 μm and (c) L_c = 35 μm. The other parameters are chosen as d = 2.6 μm, D = 5 μm, L_t = 10 μm, λ = 1.55 μm, n_{core} = 1.444. In (b) and (c), the upper graphs show cross-sections in the x-z plane for y = 0, the lower graph show cross-sections in the x-y plane at the contact point to the substrate (middle of the microfiber) and at the exit of the microfiber.

we checked the importance of the length on the transmission. Furthermore, to simulate the situation where the microfiber is lying on the substrate, we modify our model by adding a straight microfiber section between the curved fiber sections. It is shown that the addition of the straight fiber section does not reduce the transmission when the microfiber diameter is optimized. The case where the structure is covered by a cladding material is also discussed, and it is found that for both the MgF_2 substrate and the fluorosilicate glass substrate there is a length for which the transmission is minimal. The minimum transmission occurs when the microfiber is short enough (and therefore sharply bent) to show significant bending loss but too long for a significant part of the input light to be launched straight into the output taper.

This work was supported by the National Natural Science Foundation of China under Grant No. 60678039. We thank Dr. Gerhard Shoetz from Heraeus GmbH and our colleague Prof. Jianjun He for useful discussions. [a]Present address: University of California in Los Angeles, Engineering IV Building, Room 63-109, 420 Westwood Plaza, Los Angeles, CA 90095-1594, USA; [b]Present address: Data Storage Division, 5, Engineering Drive I (Off Kent Ridge Crescent, NUS), Singapore 117608, Singapore.

References

1. G. Brambilla, F. Xu, P. Horak, Y. Jung, F. Koizumi, N. P. Sessions, E. Koukharenko, X. Feng, G. S. Murugan, J. S. Wilkinson, and D. J. Richardson, Adv. Opt. Photon. **1,** 107 (2009).
2. L. Tong, R. R. Gattass, J. B. Ashcom, S. He, J. Lou, M. Shen, I. Maxwell, and E. Mazur, Nature **426,** 816 (2003).
3. G. Brambilla, V. Finazzi, and D. J. Richardson, Opt. Express **12,** 2258 (2004).
4. L. Tong, L. Hu, J. Zhang, J. Qiu, Q. Yang, J. Lou, Y. Shen, J. He, and Z. Ye, Opt. Express **14,** 82 (2006).
5. A. M. Clohessy, N. Healy, D. F. Murphy, and C. D. Hussey, Electron. Lett. **41,** 954 (2005).
6. G. Brambilla, F. Xu, and X. Feng, Electron. Lett. **42,** 517 (2006).
7. J. Bures and R. Ghosh, J. Opt. Soc. Am. A **16,** 1992 (1999).
8. K. Huang, S. Yang, and L. Tong, Appl. Opt. **46,** 1429 (2007).
9. G. Vienne, P. Grelu, X. Pan, Y. Li, and L. Tong, J. Opt. A: Pure Appl. Opt. **10,** 025303 (2008).
10. G. Vienne, Y. Li, L. Tong, and P. Grelu, Opt. Lett. **33,** 1500 (2008).
11. S. Leon-Saval, T. Birks, W. Wadsworth, P. St. J. Russell, and M. Mason, Opt. Express **12,** 2864 (2004).
12. M. A. Foster, A. C. Turner, M. Lipson, and A. L. Gaeta, Opt. Express **16,** 1300 (2008).
13. X. Jiang, L. Tong, G. Vienne, X. Guo, A. Tsao, Q. Yang, and D. Yang, Appl. Phys. Lett. **88,** 223501 (2006).
14. L. Tong, J. Lou, R. R. Gattass, S. He, X. Chen, L. Liu, and E. Mazur, Nano Lett. **5,** 259 (2005).
15. Y. Li and L. Tong, Opt. Lett. **33,** 303 (2008).
16. Y. Wu, Y.-J. Rao, Y.-H. Chen, and Y. Gong, Opt. Express **17,** 18142 (2009).
17. G. Vienne, Y. Li, and L. Tong, IEICE Trans. Electron. **E90-C,** 415 (2007).
18. F. Xu and G. Brambilla, Opt. Lett. **32,** 2164 (2007).
19. G. Vienne, Y. Li, and L. Tong, IEEE Photon. Technol. Lett. **19,** 1386 (2007).
20. S. D. Gedney, IEEE Trans. Antennas Propag. **44,** 1630 (1996).
21. MgF_2 optical properties can be found at the Refractive Index Database http://refractiveindex.info.
22. "Highly fluorine doped rods" Products information of Heraeus: http://specialty-fiber.heraeus-quarzglas.com/en/products/fluosilrods/fluosil_rods_38913.aspx (Aug. 17, 2009).
23. M. Sumetsky, Y. Dulashko, and M. Fishteyn, in *OSA Technical Digest Series (CD) of Optical Fiber Communication Conference and Exposition and The National Fiber Optic Engineers Conference* PDP46 (2007).